Available online at www.sciencedirect.com
SCIENCE DIRECT®
Thermochimica Acta 435 (2005) 222–229
thermochimica acta
www.elsevier.com/locate/tca

Analysis of magnetic and structural phase transition behaviors of $La_{1-x}Sr_xCrO_3$ for preparation of phase diagram

Fumihiko Nakamura [a], Yuhta Matsunaga [a], Norifumi Ohba [a], Kenta Arai [a], Hiroyuki Matsubara [a], Hiroki Takahashi [b], Takuya Hashimoto [a,*]

[a] *Department of Integrated Sciences in Physics and Biology, College of Humanities and Sciences, Nihon University, 3-25-40 Sakurajousui, Setagaya-ku, Tokyo 156-8550, Japan*
[b] *Department of Physics, College of Humanities and Sciences, Nihon University, 3-25-40 Sakurajousui, Setagaya-ku, Tokyo 156-8550, Japan*

Received 10 February 2005; received in revised form 29 May 2005; accepted 7 June 2005
Available online 12 July 2005

Abstract

The phase transition behavior of perovskite-type compounds, $La_{1-x}Sr_xCrO_3$, was investigated by differential scanning calorimetry (DSC), dilatometry, dc magnetic susceptibility measurement and X-ray diffraction analysis. Both second-order magnetic phase transition from antiferromagnetic to paramagnetic and first-order structural phase transition from orthorhombic to rhombohedral were observed in the DSC or dilatometric curve of every specimen. The temperatures of both these magnetic and structural phase transitions decreased linearly with an increase in Sr content. The structural phase transition temperature of $La_{1-x}Sr_xCrO_3$ with x less than 0.11 is higher than the magnetic phase transition temperature; however, a larger decrease in structural phase transition temperature than in magnetic phase transition temperature was observed with an increase in Sr content, resulting in a structural phase transition temperature lower than the magnetic phase transition temperature for $La_{1-x}Sr_xCrO_3$ with x of more than 0.12. It was also observed that the heat of absorption of the structural phase transition decreased with an increase in x. In the dependence of dc magnetic susceptibility on temperature, variations by not only magnetic but also structural phase transitions were observed. It was also revealed that thermal expansion coefficient is affected not only by structural phase transition but also magnetic phase transition. Magnetic and structural phase diagram of $La_{1-x}Sr_xCrO_3$, suggesting the existence of two Sr contents and temperatures at which triple phases coexist, was proposed.
© 2005 Elsevier B.V. All rights reserved.

Keywords: $La_{1-x}Sr_xCrO_3$; DSC; Dilatometry; Magnetic property; Phase transition; Phase diagram

1. Introduction

$La_{1-x}Ae_xMO_3$ (Ae, alkaline earth; M, 3d transition metal) with a distorted perovskite structure has attracted much interest owing to its unique property such as colossal magnetic resistance and potential application to new energy conversion devices such as solid oxide fuel cells (SOFC) [1,2]. Some $La_{1-x}Ae_xMO_3$ compounds show magnetic and/or structural phase transition. For example, $LaCrO_3$ shows magnetic phase transition from antiferromagnetic to paramagnetic and structural phase transition from an orthorhombic distorted perovskite to a rhombohedral distorted one at 15 and 240 °C, respectively [3–5]. The magnetic phase transition should be considered for application to magnetic devices. The structural phase transition should be taken into consideration for application to high-temperature device such as SOFC since discontinuous volume decrease at the structural phase transition might cause mechanical destruction. For practical applications, the partial substitution of divalent ions, such as Ca^{2+} or Sr^{2+} to La^{3+}, has been examined to control not only the electrical and/or magnetic property but also the behavior of phase transition. Sakai and coworkers performed X-ray diffrac-

* Corresponding author. Tel.: +81 3 3329 1151x5516; fax: +81 3 5317 9432.
E-mail address: takuya@chs.nihon-u.ac.jp (T. Hashimoto).

0040-6031/$ – see front matter © 2005 Elsevier B.V. All rights reserved.
doi:10.1016/j.tca.2005.06.005

tion analysis, neutron diffraction analysis, dc susceptibility measurement, differential scanning calorimetry and adiabatic calorimetry of $La_{1-x}Ca_xCrO_3$ and concluded that structural phase transition temperature increases with increasing Ca content, whereas magnetic phase transition temperature decreases [6–8]. For Sr-substituted specimens, Hayashi et al. measured dilatometry and observed a decrease in structural phase transition temperature with increasing x. They insisted that magnetic phase transition is successfully observed with a variation in thermal expansion coefficient and concluded that its temperature slightly decreased with Sr content [9]. Tezuka et al. carried out neutron diffraction analysis and dc magnetic susceptibility measurement of $La_{1-x}Sr_xCrO_3$. They observed a decrease in Neel temperature with increasing Sr content and insisted that structural phase transition temperature decreases with increasing Sr content despite the fact that the low-temperature neutron diffraction measurement was performed only on $La_{0.85}Sr_{0.15}CrO_3$ [10]. Since their specimens employed were limited at $x = 0.00$, 0.10, 0.20 and 0.30 for Hayashi et al. and at $x = 0.00$, 0.05, 0.10, 0.15, 0.20 and 0.25 for Tezuka et al., the phase diagram of $La_{1-x}Sr_xCrO_3$, which is essential for the design of materials, has not yet been proposed. One of the probable reasons for the limitation of the number of their specimens is that their experimental methods such as neutron diffraction analysis, dc magnetic susceptibility measurement and dilatometry require either a large amount of specimens or a long time for measurement. Another probable reason is that they prepared their specimens by the solid-state reaction method, in which precise control of Sr content and preparation of homogeneous specimens are difficult. In this study, successfully prepared $La_{1-x}Sr_xCrO_3$ polycrystalline powders with $x = 0.00$, 0.05, 0.10, 0.11, 0.12, 0.13, 0.14 and 0.15 by the Pechini method [11] were employed for differential scanning calorimetry (DSC), which required a far smaller amount of specimens and a shorter measurement time, to analyze the feature of transition behavior and to propose the phase diagram. On the basis of the proposed phase diagram, the effect of structural phase transition on magnetic property has been investigated. Also analyzed was the influence of magnetic phase transition on structural property, such as thermal expansion behavior.

2. Experimental

$La_{1-x}Sr_xCrO_3$ polycrystalline specimens with $x = 0.00$, 0.05, 0.10, 0.11, 0.12, 0.13, 0.14 and 0.15 were prepared from La_2O_3 (99.9%, Furuuchi Chem. Co. Ltd.), $SrCO_3$ (99.9%, Furuuchi Chem. Co. Ltd.) and $Cr(NO_3)_3{\cdot}9H_2O$ (99.9%, Wako Chem. Co. Ltd.). Prior to the preparation, La_2O_3 was heated in air at 1200 °C for 12 h in air to decompose trace amounts of impurities such as $La(OH)_3$ and $La_2(CO_3)_3$ and $SrCO_3$ was dried at 120 °C for 6 h in air. Raw materials in a stoichiometric ratio were completely dissolved in dilute nitric acid. Then, excess citric acid was added to the solution to obtain the chelate of each metal. Posterior to addition of excess ethylene glycol, the solution was heated at about 300 °C. The solution changed to a polyester resin, which was burned to a powder. The obtained powder was calcined at 750 °C for 7 h in air and pressed into pellets, which were successively sintered at 1400 °C for 17 h in air. To obtain a single-phase homogeneous specimen, the obtained pellets were reground into a powder and pressed into pellets again, which were sintered at 1400 °C for 24 h in air. For differential scanning calorimetry (DSC) and X-ray diffraction analysis, the obtained pellets were again reground to a powder. X-ray diffraction patterns (Cu Kα: 50 kV, 250 mA, Rigaku RINT-2500) indicated that the obtained specimens were of single phase with a crystal system of distorted perovskite.

To observe phase transition behavior, DSC curves of $La_{1-x}Sr_xCrO_3$ in the temperature range from −150 to 450 °C were measured at a heating rate of 10 K/min using a Rigaku DSC8230 apparatus. About 40 mg of the powder specimen crimped in an Al pan and Al_2O_3 powder also crimped similarly were employed as sample and reference, respectively. The measurements were carried out in static Ar atmosphere with an oxygen partial pressure of about 10^{-4} atm. It has been confirmed by thermogravimetry that oxygen nonstoichiometry is not induced in $La_{1-x}Sr_xCrO_3$ under this oxygen partial pressure at temperatures less than 450 °C [12,13]. Phase transition behavior was also analyzed by dilatometry using a Rigaku TMA8310 apparatus. The sintered cylindrical specimen of 4.8–5.0 mm diameter and about 12–18 mm height was used as measurement sample. SiO_2 was used as push rod and reference. The measurements were performed in air at a heating rate of 10 K/min in the temperature range of −150 to 450 °C. To analyze the feature of the phase transition thus observed, powder X-ray diffraction patterns at various temperatures and temperature dependence of magnetic dc susceptibility were measured. Powder X-ray diffraction patterns were obtained in the temperature ranges of −100 to 10 °C and 20–300 °C using MX18HF, MAC Science Co. Ltd. (Cu Kα, 60 kV, 300 mA) equipped with a refrigerator and Rigaku RINT-2500 (Cu Kα, 50 kV, 250 mA) with an electric furnace, respectively. DC magnetic susceptibility was measured with a SQUID magnetometer (Quantum Design MPMS model) after zero field cooling in the temperature ranges of −271 to 100 °C. The external magnetic field was 2 kOe. For $La_{0.87}Sr_{0.13}CrO_3$, the dependence of magnetization on the external magnetic field between −70 and 70 kOe was measured at several temperatures to analyze the magnetic property.

3. Results and discussion

3.1. Preparation of phase diagram of $La_{1-x}Sr_xCrO_3$

Fig. 1 shows the DSC curves of $La_{1-x}Sr_xCrO_3$ obtained in this study. For DSC curve of $LaCrO_3$, the endothermic peak represented by the downward arrow and the baseline

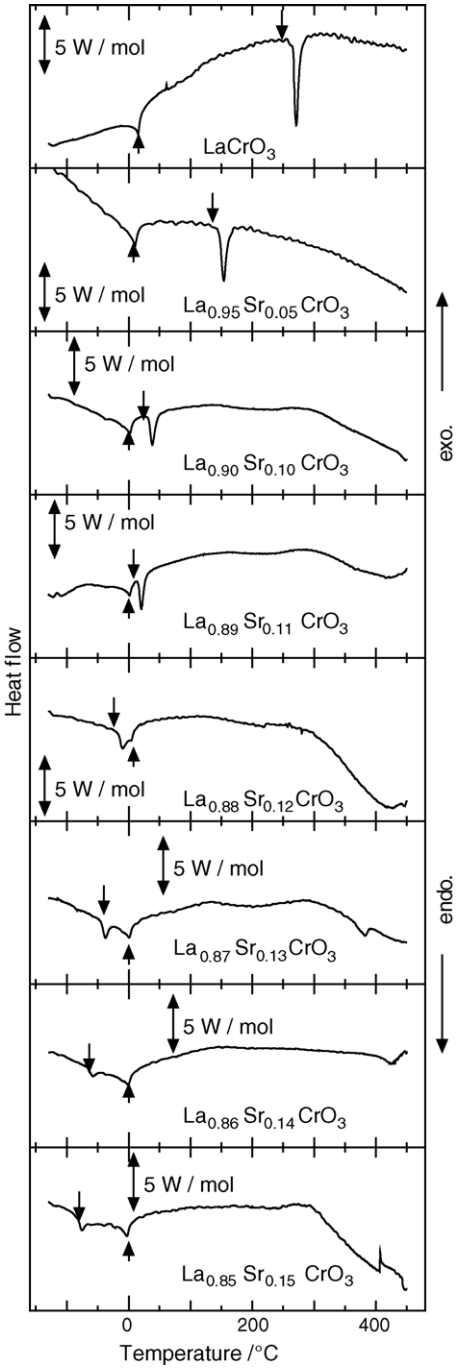

Fig. 1. DSC curves of $La_{1-x}Sr_xCrO_3$ under 1 atm. The endothermic peak represented by the downward arrow and baseline shift denoted by the upward arrow were observed in every specimen.

shift denoted by the upward arrow were observed at 256 and 14 °C, respectively. The former signal corresponded to the first-order structural phase transition from orthorhombic distorted perovskite to rhombohedral distorted perovskite, whereas the latter signal to the second-order magnetic phase transition [4,5]. Both signals were clearly observed in every $La_{1-x}Sr_xCrO_3$ for the first time. From the peak area, the variation in enthalpy, ΔH, of the first-order phase transition was calculated and depicted in Fig. 2. It was suspected that since ΔH decreased monotonically with Sr content and was as low as 32 J/mol at $x = 0.15$, the detection of ΔH by DSC in $La_{1-x}Sr_xCrO_3$ system has not been reported thus far. Both transition temperatures also decreased with an increase in Sr content. Because of the larger decrease in transition temperature for the first-order phase transition than that for the second-order phase transition, the temperature for the first-order phase transition was higher than that for the second-order phase transition of the specimens with x smaller than 0.11, whereas the reversal of transition temperature was observed for x larger than 0.12.

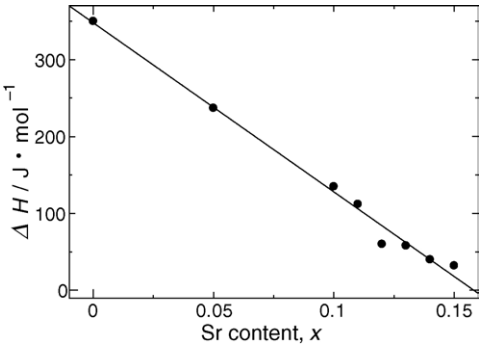

Fig. 2. Variation in enthalpy (ΔH) in first-order transition of $La_{1-x}Sr_xCrO_3$. ΔH was calculated from the peak area in DSC curves.

For the analysis of the feature of the phase transition, X-ray diffraction patterns were measured at various temperatures. Fig. 3 shows the X-ray diffraction patterns of $LaCrO_3$ at 200 and 300 °C. All peaks were indexed according to the crystal symmetry deduced from peaks in the 2θ range of 67–69°. Three peaks indexed as 0 4 0, 2 2 4 and 4 0 0 should be observed in this range for the orthorhombic symmetry, whereas two peaks as 2 2 0 and 2 0 8 for the rhombohedral symmetry. It was revealed that the crystal systems of $LaCrO_3$ were orthorhombic below 200 °C and rhombohedral above 300 °C, showing agreement with the transition temperature measured as the endothermic peak of DSC curve. Figs. 4–6 show X-ray diffraction patterns of $La_{1-x}Sr_xCrO_3$ at various temperatures. It was concluded that the endothermic peak

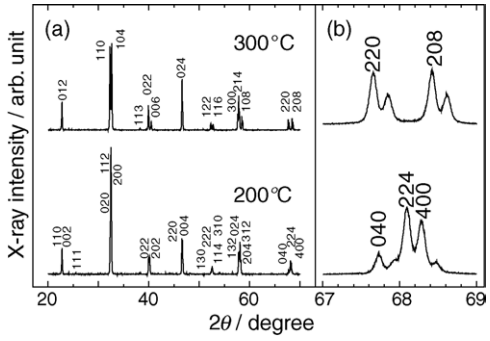

Fig. 3. X-ray diffraction patterns of $LaCrO_3$ at 200 and 300 °C in 2θ ranges of (a) 20–70° and (b) 67–69°. The diffraction patterns at 200 and 300 °C could be indexed as orthorhombic and rhombohedral, respectively.

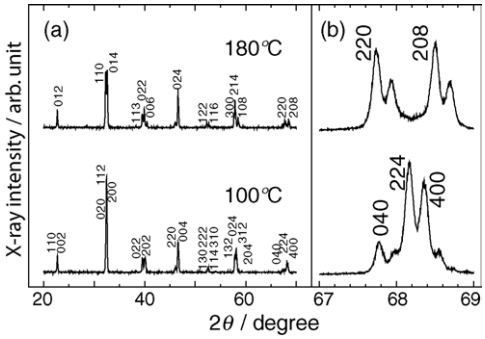

Fig. 4. X-ray diffraction patterns of $La_{0.95}Sr_{0.05}CrO_3$ at 100 and 180 °C in 2θ ranges of (a) 20–70° and (b) 67–69°. The diffraction patterns at 100 and 180 °C could be indexed as orthorhombic and rhombohedral, respectively.

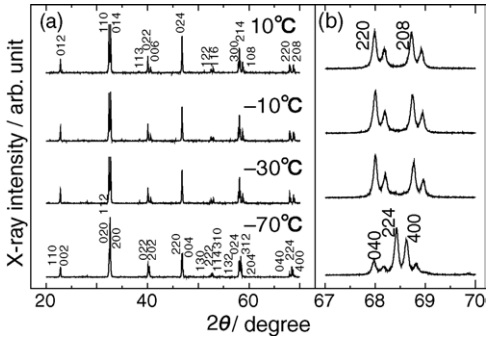

Fig. 5. X-ray diffraction patterns of $La_{0.87}Sr_{0.13}CrO_3$ at −70, −30, −10 and 10 °C in 2θ ranges of (a) 20–70° and (b) 67–70°. The diffraction patterns below −70 °C and above 30 °C could be indexed as orthorhombic and rhombohedral, respectively.

of the DSC curve depicted in Fig. 1 indicated structural phase transition from orthorhombic to rhombohedral since orthorhombic and rhombohedral symmetries were observed below and above the temperature of the endothermic peak, respectively. It was also revealed from Figs. 5 and 6 that the crystal system did not change at the temperature for the second-order phase transition observed with the baseline shift of DSC curves.

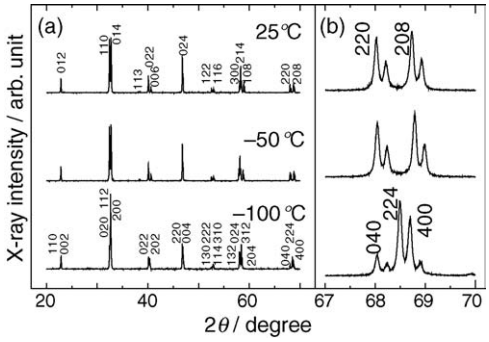

Fig. 6. X-ray diffraction patterns of $La_{0.85}Sr_{0.15}CrO_3$ at −100, −50, and 25 °C in 2θ ranges of (a) 20–70° and (b) 67–70°. The diffraction patterns below −100 °C and above −50 °C could be indexed as orthorhombic and rhombohedral, respectively.

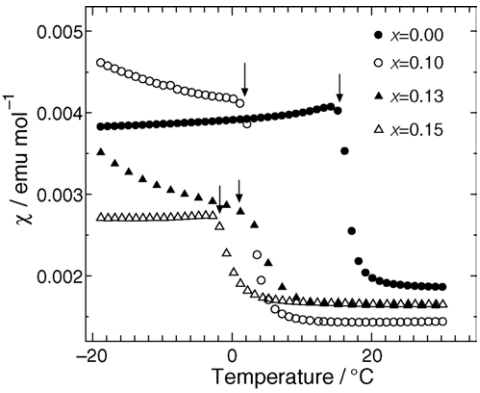

Fig. 7. DC magnetic susceptibilities of $La_{1-x}Sr_xCrO_3$ ($x = 0.00$, 0.10, 0.13, 0.15) measured after zero field cooling (ZFC). A discrete decrease in magnetic susceptibility was observed as shown by arrows.

To clarify the origin of the baseline shift of the DSC curve observed in Fig. 1, the dependence of dc magnetic susceptibility on temperature was measured and results are shown in Fig. 7. At the temperatures where the second-order phase transition was observed in DSC curves, a discrete variation in magnetic susceptibility was observed. Fig. 8 shows a variation in the magnetization of $La_{0.87}Sr_{0.13}CrO_3$ on external magnetic field at (a) 27 °C, (b) −30 °C and (c) −70 °C. At 27 °C, which was higher than second-order phase transition

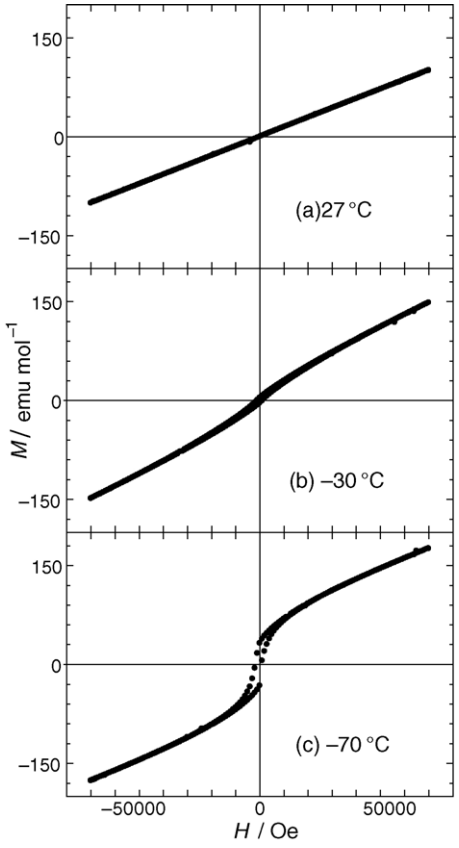

Fig. 8. Magnetic hysteresis curves of $La_{0.87}Sr_{0.13}CrO_3$ at (a) 27 °C, (b) −30 °C, and (c) −70 °C.

temperature, a linear relationship indicating a paramagnetic property was observed. At temperatures lower than second-order phase transition temperature, such as −30 and −70 °C, a hysteresis curve was obtained showing a canted antiferromagnetic property. Thus, it was concluded that the second-order phase transition observed in the DSC curve could be attributed to magnetic phase transition from antiferromagnetic to paramagnetic.

In Fig. 9, results described above were arranged as a phase diagram of $La_{1-x}Sr_xCrO_3$. Structural phase transition temperature and magnetic phase transition temperature, so called Neel temperature, were represented by closed and open circles, respectively. Four phases, i.e. (a) paramagnetic orthorhombic, (b) canted antiferromagnetic orthorhombic, (c) canted antiferromagnetic rhombohedral and (d) paramagnetic rhombohedral, were observed. Apparently, a quadruple point was observed for the specimen with $x = \sim 0.111$ at about 0.3 °C; however, it contradicted the phase rule. At the quadruple point, all the parameters, i.e., temperature, composition and pressure, should be uniquely determined since the degree of freedom f should be 0 according to the phase rule described as

$$f = c - p + 2,$$

where p denotes the number of phases. Since the $La_{1-x}Sr_xCrO_3$ system can be regarded as a two-component system of $LaCrO_3$ and Sr, the number of components c is 2. Since it is not guaranteed that the pressure (1 atm.) under which the measurements were carried out, is equal to the pressure of the quadruple point, it is probable that no quadruple point was successfully obtained in our experiment. Therefore, we suspect that the phase diagram near $x = \sim 0.011$ around 0.3 °C shown as an inset of Fig. 9 indicates two types of triple point bounded by a curve with a double-phase boundary.

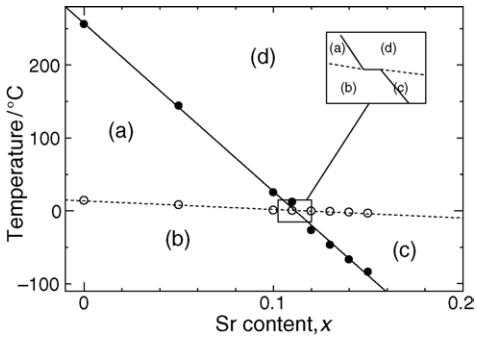

Fig. 9. Variation in phase transition temperatures with Sr content in $La_{1-x}Sr_xCrO_3$ from DSC curves. Structural transition temperatures are shown by a solid line and magnetic transition temperatures are indicated by a dotted line: (a) paramagnetic orthorhombic, (b) canted antiferromagnetic orthorhombic, (c) canted antiferromagnetic rhombohedral and (d) paramagnetic rhombohedral.

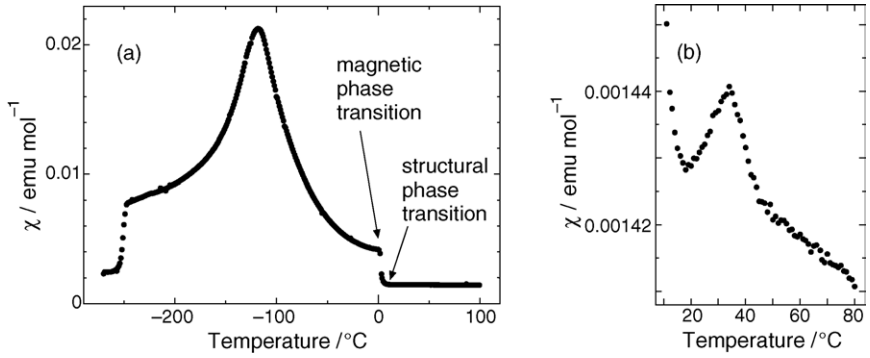

Fig. 10. Magnetic susceptibilities of $La_{0.90}Sr_{0.10}CrO_3$: (a) temperature range from −273 to 100 °C; (b) nearby structural transition temperature.

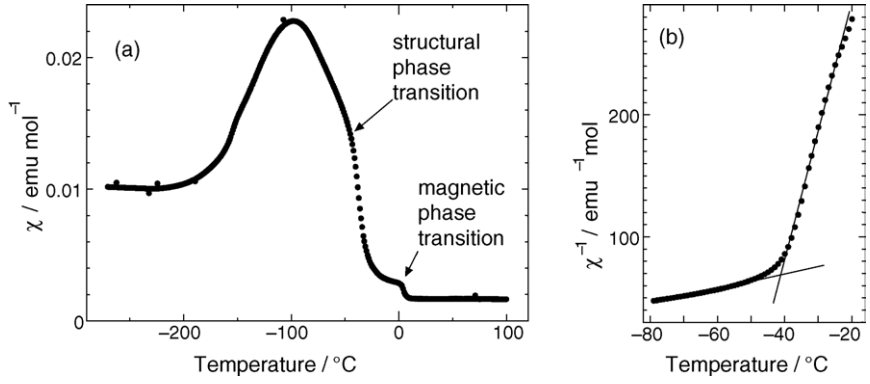

Fig. 11. (a) Magnetic susceptibility of $La_{0.87}Sr_{0.13}CrO_3$; (b) reciprocal of χ near structural transition temperature.

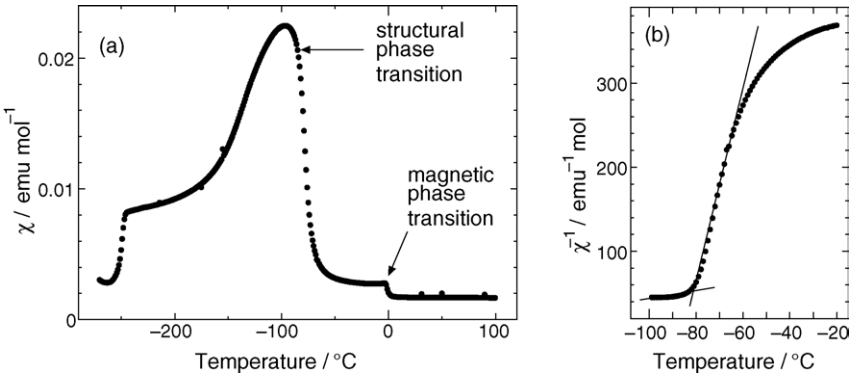

Fig. 12. (a) Magnetic susceptibility of $La_{0.85}Sr_{0.15}CrO_3$; (b) reciprocal of χ near structural transition temperature.

3.2. *Effect of structural phase transition on magnetic property*

According to Fig. 9, there exist two types of paramagnetic phase, one is orthorhombic and the other rhombohedral in $La_{1-x}Sr_xCrO_3$ with x less than 0.11. In the specimens with x larger than 0.12, two types of canted antiferromagnetic phase with different crystal structures are observed. It can be considered that a variation in crystal structure affects the magnetic property of $La_{1-x}Sr_xCrO_3$; however, there is as yet no report on the effect of structural phase transition on magnetic property. On the basis of the proposed phase diagram, we have analyzed the magnetic property of $La_{1-x}Sr_xCrO_3$ and revealed that magnetic property is influenced by crystal structure.

Fig. 10(a) shows the temperature dependence of the dc magnetic susceptibility of $La_{0.90}Sr_{0.10}CrO_3$. A discrete variation in magnetic susceptibility due to magnetic phase transition was observed at 0.6 °C. Since structural phase transition exists at 25 °C in this specimen, the magnetic susceptibility at around 25 °C was enlarged and is depicted in Fig. 10(b). The bending point was observed at the 19 °C, indicating that paramagnetic property was affected by structural phase transition from orthorhombic to rhombohedral. The magnetic susceptibility of the rhombohedral phase was slightly smaller than that of paramagnetic orthorhombic phase.

Figs. 11(a) and 12(a) show the dependence of dc magnetic susceptibility on temperature for $La_{0.87}Sr_{0.13}CrO_3$ and $La_{0.85}Sr_{0.15}CrO_3$. The influence of structural phase transition should be observed from the canted antiferromagnetic property of the specimens. From Fig. 9, the temperatures for structural phase transition are −47 and −84 °C for $La_{0.87}Sr_{0.13}CrO_3$ and $La_{0.85}Sr_{0.15}CrO_3$, respectively. Figs. 11(b) and 12(b) show the relationship between temperature and the reciprocal of magnetic susceptibility around the structural phase transition temperature of $La_{0.87}Sr_{0.13}CrO_3$ and $La_{0.85}Sr_{0.15}CrO_3$, respectively. Both data could approximately be reproduced by two types of linear relationships with crossing at the structural phase transition temperature. This result suggests that the energy for the antiferromagnetic interaction between electron spins among Cr ions is influenced by crystal structure. The temperature dependence of magnetic susceptibility in the canted antiferromagnetic rhombohedral phase was larger than that in the orthorhombic phase, suggesting that the tilting mode and angle of CrO_6 octhahedra affect the interaction of electron spins among Cr

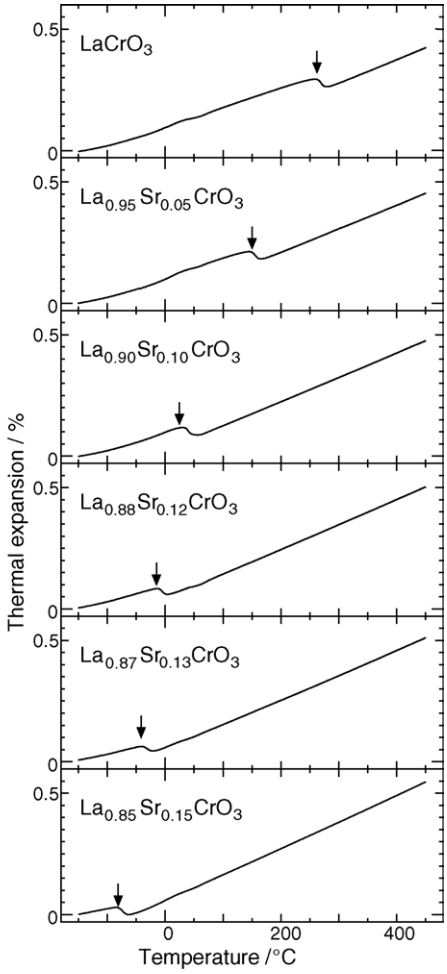

Fig. 13. Thermal expansion behavior of sintered $La_{1-x}Sr_xCrO_3$ specimens. Shrinkage due to first-order structural phase transition represented by the downward arrow is observed in every specimen.

ions. We regard that the determination of magnetic structure by neutron diffraction analysis is necessary for the precise analysis of the relationship between crystal structure and magnetic property.

3.3. Influence of magnetic phase transition on thermal expansion behavior

As discussed in Section 3.1, the crystal structure of $La_{1-x}Sr_xCrO_3$ is not affected by magnetic phase transition. However, the frequency of phonons can be changed by magnetic phase transition involving the transition of the electron spin configuration, resulting in a variation in thermal expansion coefficient. Fig. 13 shows the thermal expansion behavior of $La_{1-x}Sr_xCrO_3$ measured by dilatometry. A discrete decrease in length corresponding to structural phase transition was observed in every specimen. The temperature of the shrinkage agreed well with those observed as an endothermic peak with DSC depicted in Fig. 1. Fig. 14 shows the linear thermal expansion coefficient β of $La_{1-x}Sr_xCrO_3$ calculated from Fig. 13 using

$$\beta = \frac{1}{L}\left(\frac{\partial L}{\partial T}\right)_p,$$

where L denotes the length of the specimen. Beside the peak corresponding to the first-order structural phase transition, a discrete variation in β was also observed for every specimen. Since the temperature of variation in β, denoted by upward arrows agreed well with the magnetic phase transition temperature observed by DSC and dc magnetic susceptibility measurements, the β variation can be attributed to the second-order magnetic phase transition involving variations in electron spin configuration and phonon frequency.

Hayashi et al. reported the dilatometry of $La_{1-x}Sr_xCrO_3$ and insisted that they have observed magnetic and structural phase transitions as peaks in the temperature dependence of thermal expansion coefficient [9]. Their observed temperature dependence of β showed results qualitatively similar to our results, and the phase transition temperatures of $LaCrO_3$ and $La_{0.9}Sr_{0.1}CrO_3$ agreed well with our observed ones. However, they have not observed a negative thermal expansion coefficient in the phase transition of $La_{0.9}Sr_{0.1}CrO_3$, contradicting our observed thermal expansion behavior.

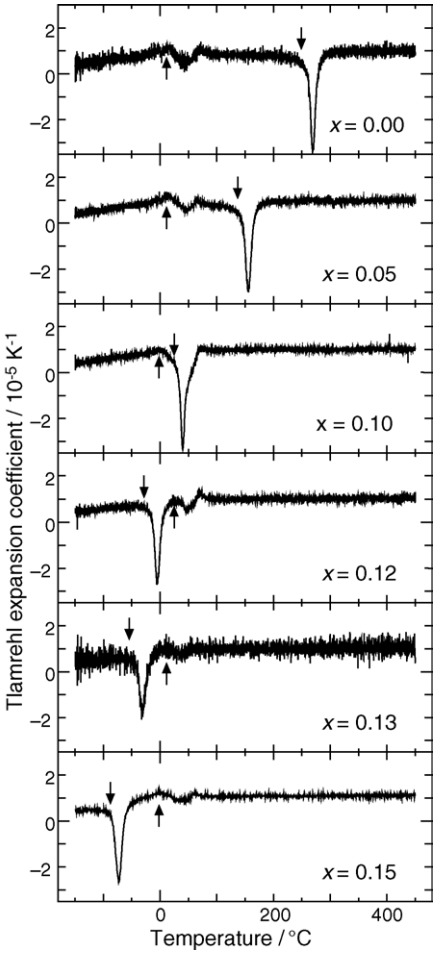

Fig. 14. Thermal expansion coefficient of sintered $La_{1-x}Sr_xCrO_3$ specimens. Shrinkage represented by the downward arrow and discontinuous variation in thermal expansion coefficient denoted by the upward arrow are observed in every specimen.

4. Conclusion

The phase transition of $La_{1-x}Sr_xCrO_3$ system was investigated by DSC, dc magnetic susceptibility measurement, X-ray diffraction analysis and dilatometry. For the first time, we successfully detected in DSC curves both structural phase transition from orthorhombic distorted perovskite and rhombohedral distorted perovskite of the first order and magnetic phase transition from canted antiferromagnetic to paramagnetic of the second order. Both transition temperatures decreased with an increase in Sr content. For specimens with x smaller than 0.11, the structural phase transition temperature was higher than the magnetic phase transition temperature, whereas it was reverse for the specimens with x larger than 0.12. A phase diagram of $La_{1-x}Sr_xCrO_3$ with two types of triple point was proposed. It was also observed that both paramagnetic and canted antiferromagnetic properties are influenced by structural phase transition and that thermal expansion coefficient is affected by magnetic phase transition.

Acknowledgments

The authors thank Dr. T. Kyomen and Prof. M. Itoh of Tokyo Institute of Technology for measurement of X-ray diffraction at low temperatures. Part of this work was supported by the “High-Tech Research Center” Project for Private Universities and a matching fund subsidy from the Ministry of Education, Culture, Sports, Science and Technology, 2000–2004.

References

[1] Y. Tokura, A. Urushibara, Y. Moritomo, T. Arima, A. Asamitsu, G. Kido, N. Furukawa, J. Phys. Soc. Jpn. 63 (1994) 3931.
[2] N.Q. Minh, J. Am. Ceram. Soc. 76 (1993) 563.
[3] H.E. Höfer, W.F. Kock, J. Electrochem. Soc. 140 (1993) 2889.
[4] S.A. Howard, J. Yan, H.U. Anderson, J. Am. Ceram. Soc. 75 (1991) 1685.
[5] N. Sakai, S. Stølen, J. Chem. Thermodyn. 27 (1995) 493.
[6] N. Sakai, J. Chem. Thermodyn. 28 (1996) 421.
[7] N. Sakai, T. Kawada, H. Yokokawa, M. Dokiya, T. Iwata, Solid State Ionics 40/41 (1990) 394.
[8] N. Sakai, H. Fjellvåg, B.C. Hauback, J. Solid State Chem. 121 (1996) 202.
[9] H. Hayashi, M. Watanabe, M. Ohuchida, H. Inaba, Y. Hiei, T. Yamamoto, M. Mori, Solid State Ionics 144 (2001) 301.
[10] K. Tezuka, Y. Hinatsu, A. Nakamura, T. Inami, Y. Shimojo, Y. Morii, J. Solid State Chem. 141 (1998) 404.
[11] M.P. Pechini, US Patent 3,330,697 (1967).
[12] T. Nakamura, G. Petzow, L.J. Gauckler, Mater. Res. Bull. 14 (1979) 649.
[13] J. Mizusaki, S. Yamauchi, K. Fueki, A. Ishikawa, Solid State Ionics 12 (1987) 119.